2018

Numerical Analysis of Friction power and Wear of Vane in Rotary Compressor

Zhong Yang
Guangdong Meizhi Compressor Co. Ltd., China, People's Republic of, yz_777@qq.com

Hong Guo
Guangdong Meizhi Compressor Co. Ltd., China, People's Republic of, zhong1.yang@chinagmcc.com

Bo Jiang
Guangdong Meizhi Compressor Co. Ltd., China, People's Republic of, jiangb@chinagmcc.com

Binsheng Zhu
Guangdong Meizhi Compressor Co.Ltd, China, People's Republic of, zhubs@chinagmcc.com

Numerical Analysis of Friction Power and Wear of Vane in Rotary Compressor

Zhong YANG[1]*, Hong GUO[2], Bo JIANG[3], Binsheng ZHU[4]

[1]Guangdong Meizhi Compressor Co.Ltd.,
Shunde, Guangdong, China
yz_777@qq.com

[2]Guangdong Meizhi Compressor Co.Ltd.,
Shunde, Guangdong, China
guoh@chinagmcc.com

[3]Guangdong Meizhi Compressor Co.Ltd.,
Shunde, Guangdong, China
jiangb@chinagmcc.com

[4]Guangdong Meizhi Compressor Co.Ltd.,
Shunde, Guangdong, China
zhubs@chinagmcc.com

ABSTRACT

In this article, a numerical method was established to analyze the friction power and wear of vane in the rotary compressor. In this method, the time domain was divided into many steps, the physical process was simplified as an explicit model. At each delta time step, three sub models were calculated iteratively, the geometric model, the contact model and the friction model. Firstly, in the geometric model, geometric kinematics of vane and piston were obtained by calculating multi body dynamical equation. Secondly, in the contact model, Reynolds equation and elastic contact equation were solved as a coupled problem to get the thickness distribution of oil film in the sliding surface. From the oil film thickness distribution, the asperity contact stress and oil film pressure could be obtained, and all other mechanical information could be calculated. Thirdly, in the friction model, the friction power and wear depth distribution were obtained. The friction power was calculated by the time integration of PV value. The PV value was calculated by substituting asperity contact stress and vane sliding velocity. The friction power was input into the Archard wear theory to get the wear depth distribution. Base on this numerical method, the friction power and wear depth distribution of vane friction pairs were got for different rotary compressors in different conditions. Some of the experiments can be replaced by this numerical method, especially the durability experiment. The parametric sensitivity analysis could be done, so, furthermore, it can offer design reference for rotary compressor.

1. INTRODUCTION

Rolling piston type rotary compressors are widely used in air conditions due to their small size, light weight, simple structure, low cost and high performance as compared with reciprocating compressors. However, they also have disadvantages. One of those is friction loss which occurs closely related to motions of vane of the compressor. When the friction loss of the vane increases, the coefficient of performance (COP) of the compressor will decrease. Due to recent environment problems represented by global warming, a demand for energy saving has been increasing rapidly. Therefor performance improvement studies of the compressor play an important role to reduce its friction power and increase the COP.

Therefore, the optimum design to get a good lubrication condition on the sliding surface of the vane is required. In order to optimize the design, the mechanics principle of the vane friction pairs must be analyzed. In recent years, much research work has been performed on the lubrication of the vane in rotary compressors [1-9]. In the literature, the oil film between vane and vane slot was simplified as a wedge plane. The reaction forces of the oil film are calculated by the numerical solution of Reynolds equation, such as Newton-Raphson method and Runge-Kutta method. The asperity contact stress and oil film pressure could be obtained. On the basis of these work, there is little further study of the friction power and the amount of wear. So, in this paper, a numerical method was established to get the friction power and wear depth distribution of rotary compressor vane on the basis of existing research.

2. GOVERNING EQUATIONS

In the compression mechanism of a rotary compressor for air conditioners, a vane is provided to separate the suction chamber and the compression chamber as Fig.1 shows. There are three main cantact friction pairs in the vane during the motion of the vane, such as vane and vane slot on suction side, vane and vane slot on discharge side, vane top and rolling piston.

In order to analyze the friction power and wear of vane in the rotary compressor, all the contact force condition should be calculated at every time step. So, a time domain algorithm as an explicit model was established. During the rotation of the crankshaft, time was divided into many steps. At each delta time step, three sub models were calculated iteratively, the geometric model, the contact model and the friction model. The result of the last submodel was entered as a initial condition into the next model, meanwhile, the result of friction model was also entered into geometric model. So, the whole model is a cyclic iteration model.

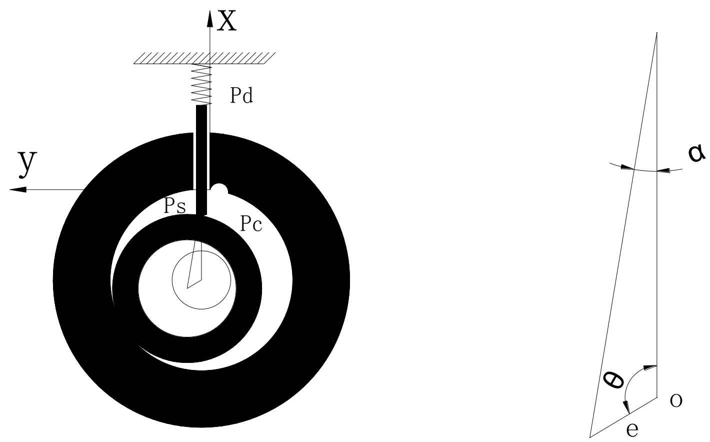

Figure.1. Brief drawing of compression mechanism in rotary compressor

2.1 Geometric mode

In the geometric model, as shown in Fig.1, geometric kinematics of vane and piston were obtained by calculating multi body dynamical equation. During the rotation of the crankshaft, the motion of the vane is clear at every moment. The displacement velocity and acceleration of the vane could be calculated by equations as follows.

$$\theta = \omega t = 2\pi f t \tag{1}$$

$$s_{va-x} = r_{\_cy} + r_{\_va} - e\cos\theta - \sqrt{(r_{\_pis\_2} + r_{\_va})^2 - (e\sin\theta)^2} \tag{2}$$

$$v_{va-x} = 2\pi f e\sin\theta + \frac{2\pi f e^2 \sin\theta\cos\theta}{\sqrt{(r_{\_pis\_2} + r_{\_va})^2 - (e\sin\theta)^2}} \tag{3}$$

$$a_{va-x} = (2\pi f)^2 e\cos\theta + \frac{(2\pi f)^2 e^2 \cos 2\theta}{\sqrt{(r_{\_pis\_2} + r_{-va})^2 - (e\sin\theta)^2}} + \frac{(2\pi f)^2 e^4 (\sin 2\theta)^2}{4\sqrt{\left[(r_{\_pis\_2} + r_{-va})^2 - (e\sin\theta)^2\right]^3}} \tag{4}$$

2.2 Contact model

2.2.1 Equilibrium equation of vane

Figure.2 shows the forces acting on the vane. Under the action of resultant force, the vane will exhibit linear acceleration and rotation acceleration in the coordinate system. The equilibrium equations of vane were listed as follows.

$$\sum F_x = -F_{vx} - F_s + F_{t-c} - F_{of-c} - F_{of-s} + F_{t-s} + F_{vt}\sin\alpha + F_{vn}\cos\alpha = m_{va}a_{va-x} \tag{5}$$

$$\sum F_y = F_{c-c} + F_{oc-c} - F_{oc-s} - F_{c-s} + F_{vy} + F_{vt}\cos\alpha - F_{vn}\sin\alpha = m_{va}a_{va-y} \tag{6}$$

$$\sum M = F_{c-c}L_{c-c} + F_{oc-c}L_{oc-c} - F_{oc-s}L_{oc-s} - F_{c-s}L_{c-s} - F_{vt}\cos\alpha\, x_{vn} + F_{vn}\sin\alpha\, x_{vn} = I_{va}\ddot{\beta} \tag{7}$$

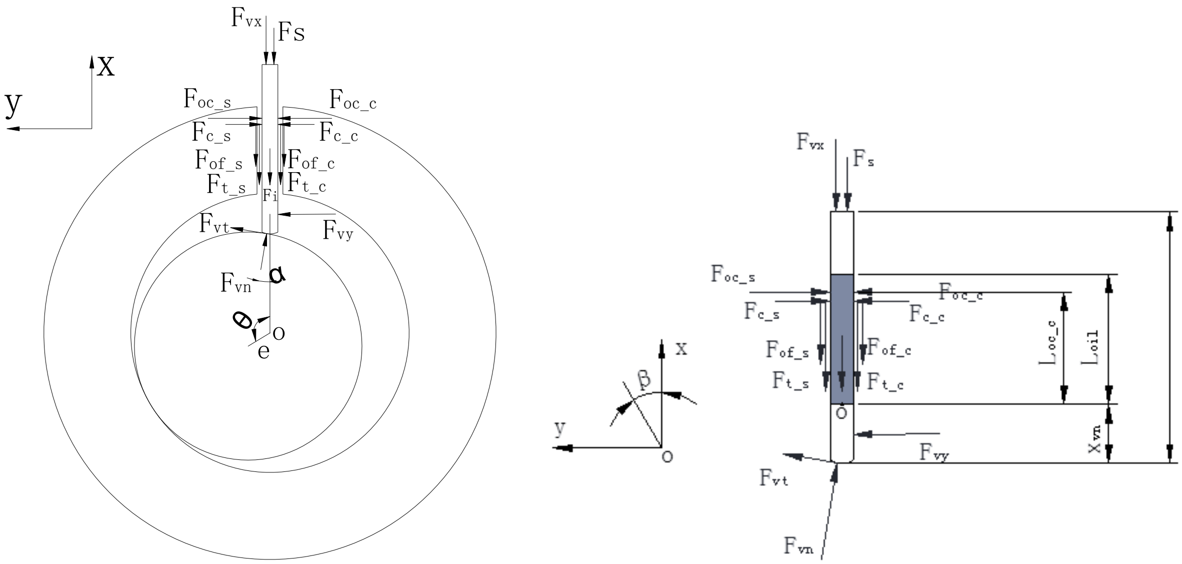

Figure.2. Forces acting on the vane

2.2.2 Reynolds equation of oil film

Figure.3 shows the coordinate system of oil film between vane and vane slot. The oil film between vane and vane slot was simplified as a wedge plane, and further simplified to a triangle. In the coordinate system, this triangle can be written as Eq.(8).

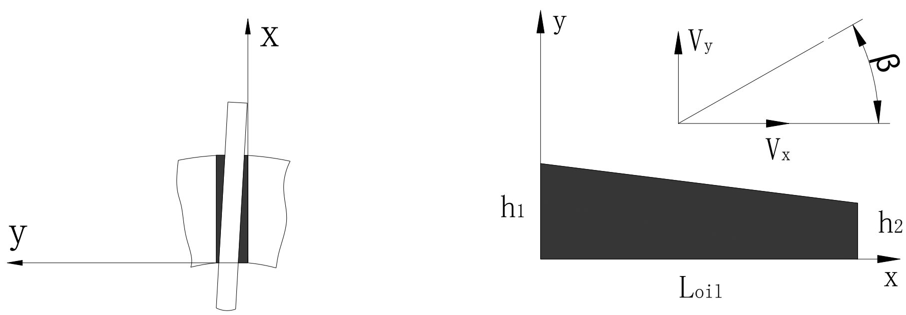

Figure.3. Coordinate system of oil film between vane and vane slot

$$h = kx + b \tag{8}$$

where, h is the thickness distribution of oil film, k ($k \approx \beta$) is slope of the oil film line, it equals to the inclination of vane. The boundary condition of oil film is expressed as follows:

$$h(x_1 = 0) = h_1\,; \qquad h(x_2 = L_{oil}) = h_2\,; \tag{9}$$

The governing equation of this one dimensional oil film pressure is the general Reynolds equation, neglecting the dependence of oil density; that is,

$$\frac{\partial}{\partial x}\left(\frac{h^3}{\eta}\frac{\partial P}{\partial x}\right) = 6v_{va-x}\frac{\partial h}{\partial x} + 12\frac{\partial h}{\partial t} \tag{10}$$

where,
$$\frac{\partial h}{\partial t} = \frac{\partial(kx+b)}{\partial t} = \frac{\partial k}{\partial t}x + \frac{\partial b}{\partial t} = \dot{\beta}x + \dot{b} = \dot{\beta}x + v_{va-y} \tag{11}$$

Substituting Eq.(8) and (11) into (10), then an analytical formula solution of Reynolds equation is obtained, the formula can be written by two cases.
Case 1, when $k = \beta \neq 0$

$$P = \dot{\beta}\frac{6\eta}{\beta^3}\left[\ln h + \frac{2b}{h} - \frac{b^2}{2h^2}\right] - \frac{(6v_{va-x}\beta\eta + 12\eta v_{va-y})}{\beta^2 h} + \frac{C_1}{h^2} + C_2 \tag{12}$$

where, C_1 and C_2 are integration constant, which are determined by the boundary condition as follows.

$$P(h = h_1) = P_1 \tag{13}$$

$$P(h = h_2) = P_2 \tag{14}$$

where, P_1 is the inlet pressure of oil film, P_2 is the outlet pressure of oil film.

Case 2, when $k = \beta = 0$

$$P = \frac{2\eta}{h^3}\dot{\beta}x^3 + \frac{6\eta}{h^3}v_y x^2 + C_3 x + C_4 \tag{15}$$

where, C_3 and C_4 are integration constant, which are determined by the boundary condition Eq.(13) and (14).

2.2.3 Asperity Contact Equation
Patir and Cheng (1978) [10] gave the asperity contact equations based on the theory which was pointed out by Greenwood and Tripp(1970) [11]. It was used to calculate the asperity contact force of the vane sliding surface between the vane and vane solt.

$$P_{solid} = K_{solid}E^* F_{\frac{5}{2}}(H_s) \tag{16}$$

$$E^* = \frac{1}{\frac{1-\gamma_1^2}{E_1} + \frac{1-\gamma_2^2}{E_2}} \tag{17}$$

$$F_{\frac{5}{2}}(H_s) = \begin{cases} 4.408610 \times 10^{-5}(4 - H_s)^{6.804} & (H_s < 4) \\ 0 & (H_s \geq 4) \end{cases} \tag{18}$$

$$H_s = \frac{h}{\sigma_s} \tag{19}$$

$$\sigma_s = \sqrt{\sigma_1^2 + \sigma_2^2} \tag{20}$$

2.3 Friction Model

Archard(1953) [12] gave a wear theory. It was used in this article to calculate the wear depth of vane. Eq.(21) shows the Archard wear volume equation. It can be translated into wear depth equation as Eq.(22).

$$V_{wear} = h_{wear} \cdot \Delta s = K_{wear}\frac{W_{wear}L_{wear}}{3\sigma_s} \tag{21}$$

$$h_{wear} = K_{wear}\frac{L_{wear}}{3\sigma_s}\frac{W_{wear}}{\Delta s} = \int_{t=0}^{t=T}\left(K_{wear}\frac{P_{solid}v_{slip}}{3\sigma_s}\right)dt = \frac{K_{wear}}{3\sigma_s}\int_{t=0}^{t=T}(P_{solid}v_{slip})\,dt \tag{22}$$

3. RESULTS AND DISCUSSION

Eq.(1)-(22) were solved as a couple problem. Analytical solutions were obtained first for all differential equations. At each delta time step, all explicit analytical equations in three models were solved by computer program. The result of the previous step was used as the initial condition of the next step. Between two adjacent time steps, time differential method was used to transmit information. Time differential equations were as follows. Firstly, the vane acceleration of previous step was calculated from Eq.(5)-(7). Then, Eq.(23)-(26) was used to calculate the displacement and velocity of vane for next step. The coupled problem becomes time variant, and is solved recursively along the time axis. By this approach, the solutions of h and k are obtained. Consequently, all other unknown physical quantities are obtained. In order to get the stable result, 4 cycles are calculated. In the fourth cycle, the result has been stabilized basically.

$$h_{n+1}^{mid} = h_n^{mid} + \dot{h}_n^{mid}\Delta t \tag{23}$$

$$\dot{h}_{n+1}^{mid} = \dot{h}_n^{mid} + \ddot{h}_n^{mid}\Delta t \tag{24}$$

$$k_{n+1} = k_n + \dot{k}_n\Delta t \tag{25}$$

$$\dot{k}_{n+1} = \dot{k}_n + \ddot{k}_n\Delta t \tag{26}$$

A typical rotary compressor was chosen as an analysis case. Its rotating frequency is 60Hz, the suction and discharge pressure is 0.36/1.90MPa. The friction coefficient at asperity contact condition between vane and vane slot is 0.15, meanwhile, the friction coefficient at asperity contact condition between vane and piston is 0.15. The equivalent viscosity of oil mixed with refrigerant gas is 1.75mPa.s. Substituting this typical rotary compressor's parameters into program, then, the results will be obtained. Fig.4 shows the pressure in compression chamber during four cycles, where, the dynamic effect of the discharge valve is neglected.

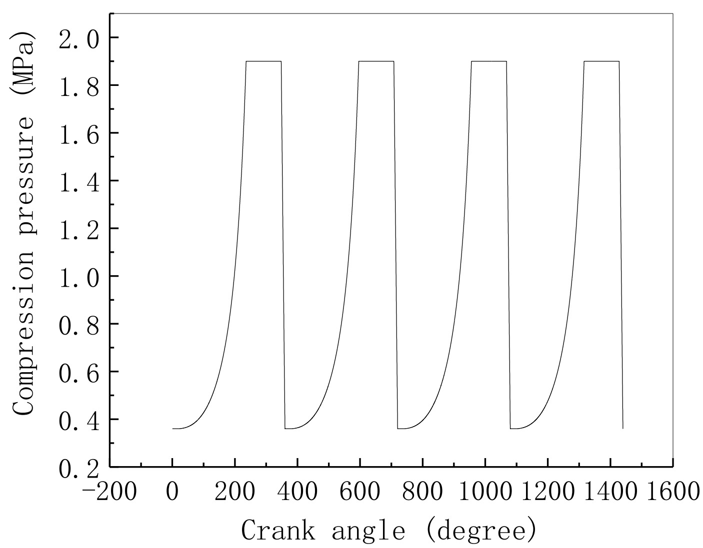

Figure.4. Pressure in compression chamber for four cycles

3.1 Contact force

Fig.5 shows the lubrication characteristics of vane sliding surfaces during four cycles. It contains minimum oil film thickness, oil film force, and asperity force. From these figures, the numerical results are unstable in the first cycle, and then, it tends to be stable in the third or fourth cycle. The asperity force appears in both vane sides. This is the main cause of friction power and wear in vane sliding surface.

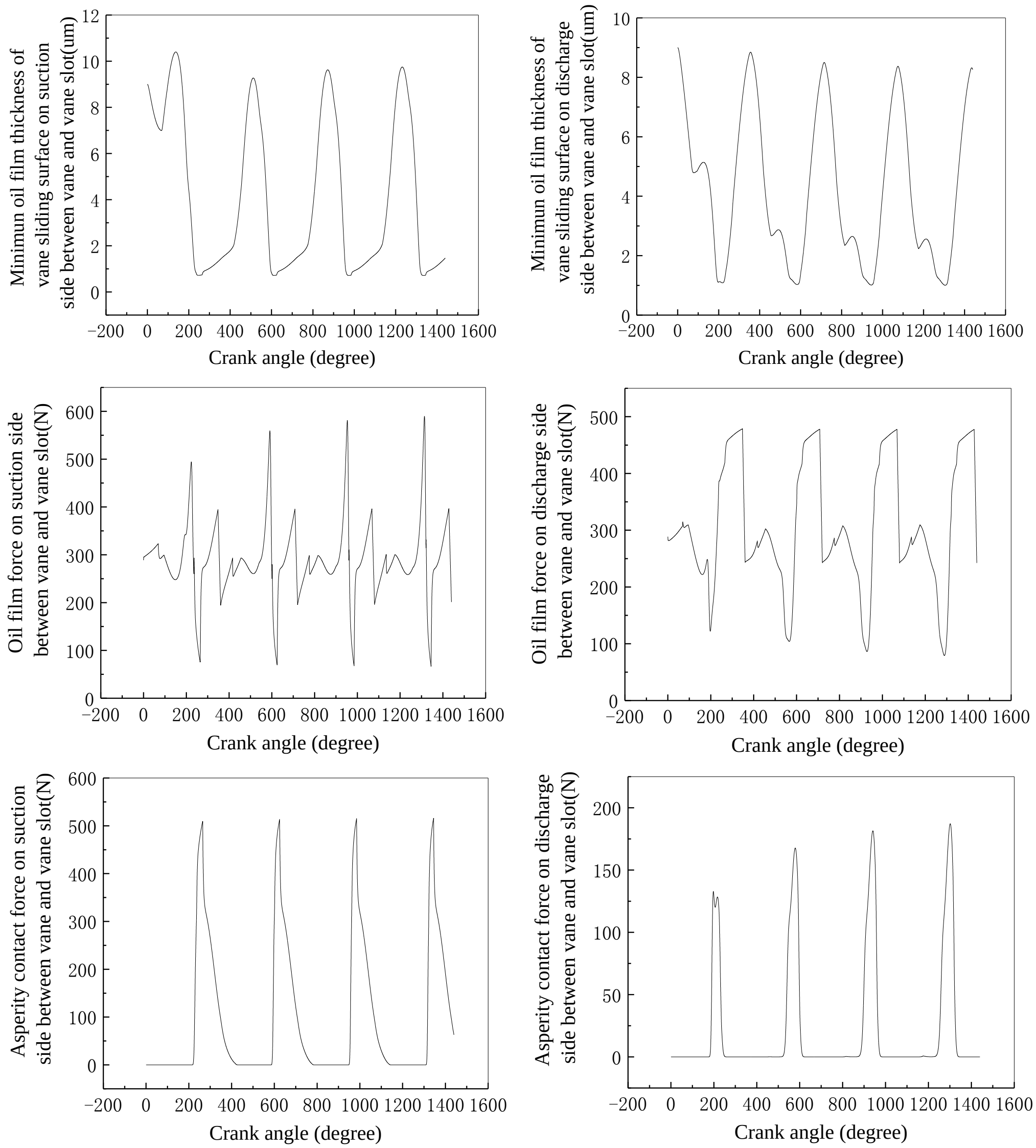

Figure.5. Lubrication characteristics of vane sliding surfaces

3.2 Friction power

Fig.6 shows the friction power of vane contact pairs during four cycles. It contains the vane top, and vane side friction power. The friction power will be dissipated with the form of heat. If the friction power could be reduced, the COP value of the rotary compressor will increase.

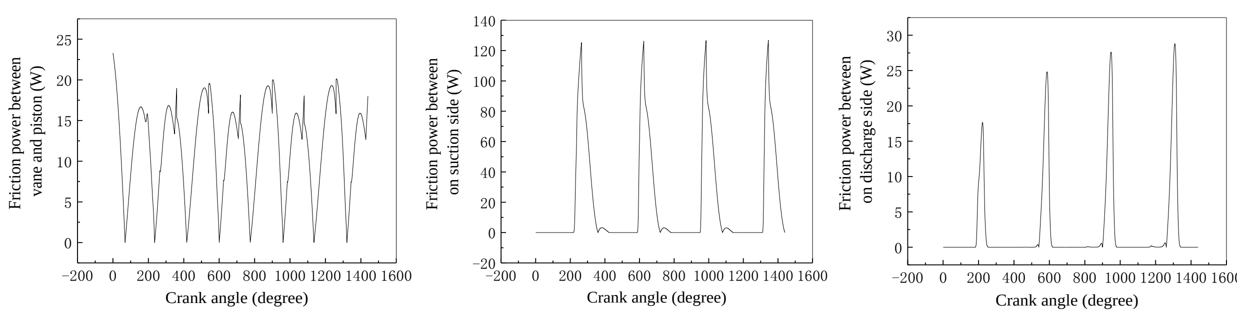

Figure.6. Friction power of vane contact pairs

3.3 Wear depth distribution

Fig.7 shows the wear depth distribution of vane and vane slot after 1000 hours durability test. In Fig.7(a), the x axis is the arc curves of the vane top, the y coordinate is the wear depth distribution. The wear of vane top is mainly concentrated in the middle area of the vane top. It is because that, there is no contact between vane top and piston on both sides of the edge due to the geometric structure relation. In Fig.7(b)-(c), the x axis is the coordinate value from the vane top to vane tail. In Fig.7(d)-(e), the x axis is the coordinate value from inside to outside of the vane slot. The y coordinate is the wear depth distribution too.

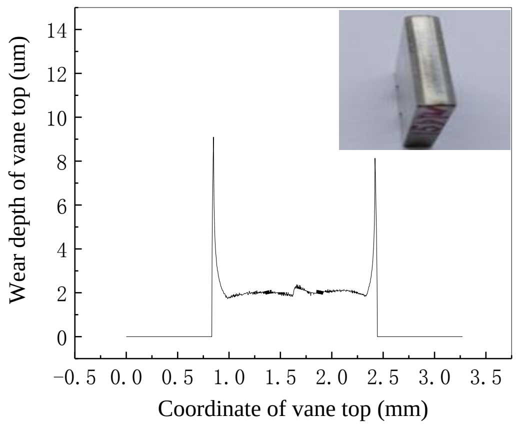

(a) Wear depth of vane top

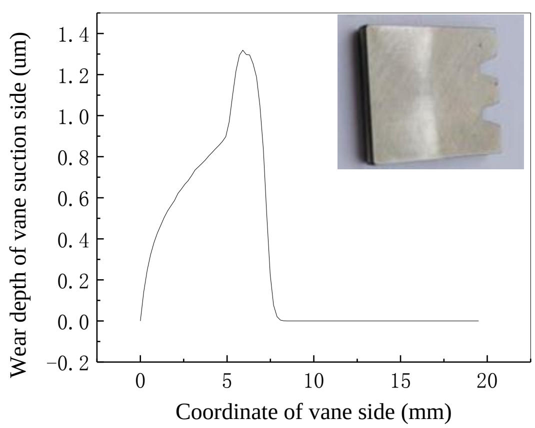

(b) Wear depth of vane suction side

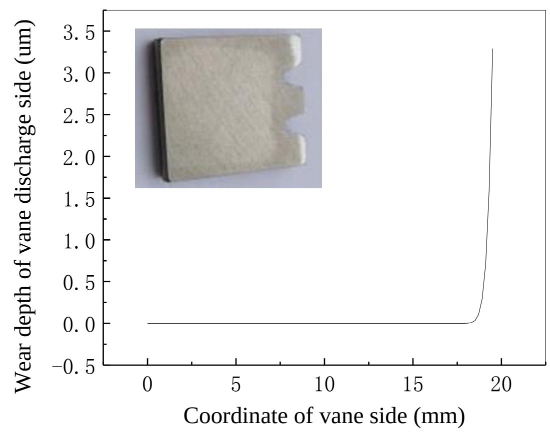

(c) Wear depth of vane discharge side

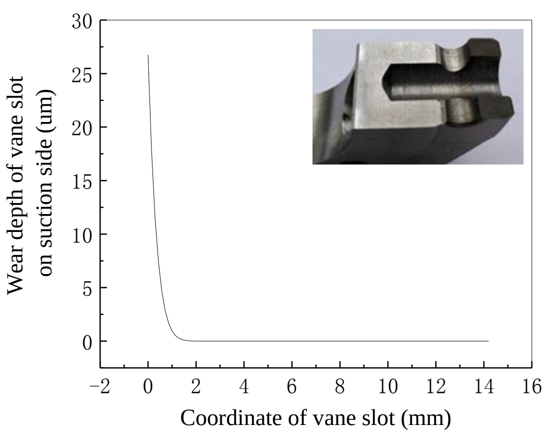

(d) Wear depth of vane slot on suction side

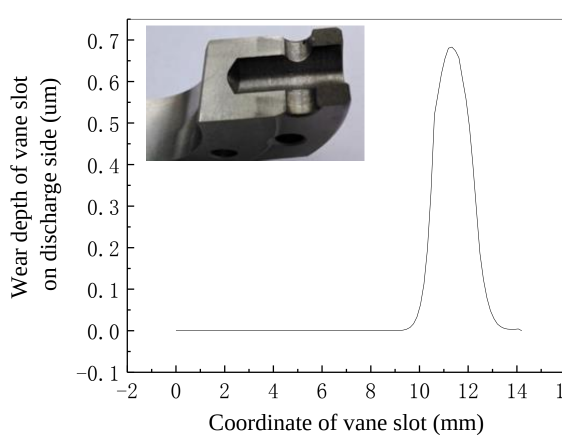

(e) Wear depth of vane slot on discharge side

Figure.7. Wear depth distribution of vane and vane slot after 1000 hours durability test by theory and experiment.

The corresponding experiments have been carried out. The wear depth depends on the wear coefficient of the materials, it can't be measured accurately. The relative distribution of wear depth is more valuable than the absolute value. The brightness in the test photos shows the relative wear depth. After 1000 hours durability test, the contrast of the wear area can be clearly seen. The cylinder is cut into two halves, so that the detail wear distribution of vane slot can be completely seen. All these numerical results in Fig.7 compare well with the experiments.

4. CONCLUSION

A numerical analysis of friction power and wear of vane in rotary compressor was established. The physical process was simplified as an explicit model. At each delta time step, three sub models were calculated iteratively. Between two adjacent time steps, time differential method was used to transmit information. At last, the friction power and wear of vane were obtained, and it compares well with the durability experiment. This numerical method can offer optimal design for rotary compressor.

NOMENCLATURE

α	: Rotated eccentricity angle, rad
β	: Vane inclination angle, rad
γ_1	: Poisson ratio of one contact material
γ_2	: Poisson ratio of anther contact material
θ	: Angle of crankshaft rotation, rad
η	: Oil viscosity, Pa s
σ_s	: Equivalent surface roughness, m
σ_1	: Roughness of one contact material, m
σ_2	: Roughness of anther contact material, m
σ_t	: Yield strength of contact material, Pa
a_{va-x}	: X direction acceleration of vane, m/s^2
a_{va-y}	: Y direction acceleration of vane, m/s^2
b	: Vane line intercept, m
e	: Eccentricity of the crankshaft, m
E^*	: Equivalent modulus, Pa
E_1	: Modulus of one contact material, Pa
E_2	: Modulus of anther contact material, Pa
f	: Crankshaft rotation frequency, Hz
F	: Equivalent concentrated force of oil film, N
F_τ	: Fluid friction force of Oil film, N
F_{vx}	: Gas pressure force on the vane end, N
F_s	: Spring force, N
F_{t-c}	: Asperity friction force on discharge side, N
F_{of-c}	: Oil viscous force on discharge side, N
F_{of-s}	: Oil viscous force on suction side, N
F_{t-s}	: Asperity friction force on suction side, N
F_{vt}	: Friction force between vane and piston, N
F_{vn}	: Normal force between vane and piston, N
F_{c-c}	: Asperity force on discharge side, N
F_{oc-c}	: Oil force on discharge side, N
F_{oc-s}	: Oil force on suction side, N
F_{c-s}	: Asperity force on suction side, N
F_{vy}	: Gas pressure force on the vane side, N
h	: Oil film thickness, m
h_1	: Oil film thickness in the inset, m
h_2	: Oil film thickness in the outset, m
h_{wear}	: Wear depth, m
H	: Vane height, m
k	: Vane inclination slope
K_{solid}	: Asperity contact coefficient
K_{wear}	: Wear coefficient
L_{wear}	: Slip distance, m
L_{oil}	: Length of oil film, m
L_{c-c}	: Distance of discharge asperity force, m
L_{oc-c}	: Distance of discharge oil force, m
L_{oc-s}	: Distance of suction oil force, m
L_{c-s}	: Distance of suction asperity force, m
M	: Equivalent moment of oil film pressure, N m
m_{va}	: Mass of the vane, N
P	: Oil film pressure, Pa
P_1	: Oil film pressure in the inset, Pa
P_2	: Oil film pressure in the outset, Pa
P_s	: Pressure in the suction chamber, MPa
P_d	: Pressure in the compression chamber, MPa
P_{solid}	: Asperity contact pressure, Pa
$r_{\_va}$	: Radius of the vane top, m
$r_{\_cy}$	: Inner radius of the cylinder, m
$r_{\_pis2}$	: External radius of the piston, m
s_{va-x}	: X direction displacement of vane, m
t	: Time, s
v_{slip}	: Slip velocity, m/s
v_{va-x}	: X direction velocity of vane, m/s
v_{va-y}	: Y direction velocity of vane, m/s
W_{wear}	: Asperity force, N
V_{wear}	: Wear volume, m^3
$\tilde{X}$	: Arm length of equivalent oil force, m
x_{vn}	: Half the length of the vane, m
Δt	: A delta time, s

REFERENCES

[1] Lichun, Hao., Yonggang, Meng., 2015, Numerical prediction of wear process of an initial line contact in mixed lubrication conditions. *Tribol Lett*, Vol. 60(2), pp.1-16.
[2] Ito, Y., Hattori, H., Miura, K., 2010, Numerical analysis for rotating motion of a rolling piston in rotary compressors-effective factors for characteristics of rotating motion of a rolling piston. International Compressor Engineering Conference at Purdue, 1217.
[3] Ito, Y., Hattori, H., Miura, K., 2014, Mixed lubrication analysis of vane sliding surface in rotary compressor mechanics – influences of friction of vane sliding surface on lubrication condition between vane top and rolling piston. International Compressor Engineering Conference at Purdue, 1296.
[4] Ito, Y., Hattori, H., Miura, K., Hirayama, T., 2006, Mixed lubrication analysis of vane sliding surface in rotary compressor mechanics. International Compressor Engineering Conference at Purdue, C137.
[5] Ito, Y., Hattori, H., Miura, K., 2008, Mixed lubrication analysis of vane sliding surface in rotary compressor mechanics – influences of elastic deformation at surface end of vane-slot. International Compressor Engineering Conference at Purdue, 1248.
[6] Fujimoto, S., Sakitani, K., Watada, M., 1984, Tribology analysis in rolling piston type compressor. International Compressor Engineering Conference at Purdue, 477, pp.377-382.
[7] Yanagisawa, T., Shimizu, T., Chu, I., Ishijima, K., 1982, Motion analysis of rolling piston in rotary compressor. International Compressor Engineering Conference at Purdue, 392, pp.185-192.
[8] Jintai, Mi., Yonggang, Meng., 2014, Numerical analyses of hydrodynamic lubrication and dynamics of the rolling piston and crankshaft in a rotary compressor. Tribology Transactions, Vol. 57, pp.1136-1147.
[9] Xingbiao, Zhou., Bo, Jiang., Shuangjian Liang., 2014, Hydrodynamic lubrication analysis of eccentric bearing in rotary compressor. International Compressor Engineeri*ng Conference at Purdue*,1110.
[10] Patir, N., Cheng, H. S., 1978, Effect of surface roughness orientation on the central film thickness in E.H.D. contacts, Proceeding of the Institute of Mechanical Engineering Part I., vol. 185, no. 48, p. 15-21.
[11] Greenwood, J. A., Tripp, J. H., 1970, The Contact of Two Nominally Flat Surfaces, Proceeding of the Institution of Mechanical Engineers., vol. 185, no. 48: p. 625-633.
[12] Archard, J. F., Contact and rubbing of flat surfaces, Journal of Applied Physics, vol. 24, no. 8, pp. 981–988, 1953.